

Photometric and spectroscopic evidence for a dense ring system around Centaur Chariklo[★]

R. Duffard¹, N. Pinilla-Alonso², J.L. Ortiz¹, A. Alvarez-Candal³, B. Sicardy⁴, P. Santos-Sanz¹, N. Morales¹, C. Colazo⁵, E. Fernández-Valenzuela¹, and F. Braga-Ribas³

¹ Instituto de Astrofísica de Andalucía - CSIC. Glorieta de la Astronomía s/n. Granada. 18008. Spain
e-mail: duffard@iaa.es

² Department of Earth and Planetary Sciences, University of Tennessee, Knoxville, TN, 37996-1410, USA

³ Observatorio Nacional de Rio de Janeiro, Rio de Janeiro, Brazil.

⁴ LESIA-Observatoire de Paris, CNRS, UPMC Univ. Paris 6, Univ. Paris-Diderot, 5 place J. Janssen, 92195 Meudon Cedex, France.

⁵ Observatorio Astronómico, Universidad Nacional de Córdoba, Laprida 854, Córdoba 5000, Argentina.

ABSTRACT

Context. A stellar occultation observed on 3rd June 2013 revealed the presence of two dense and narrow rings separated by a small gap around the Centaur object (10199) Chariklo. The composition of these rings is not known. We suspect that water ice is present in the rings, as it is the case for Saturn and other rings around the giant planets.

Aims. In this work we aim to study if the variability in the absolute magnitude of Chariklo and the temporal variation of the spectral ice feature, even its disappearance in 2007, can be explained by an icy ring system whose aspect angle changes with time.

Methods. We modeled the light reflected by a system as the one described above to explain the variations on the absolute magnitude of Chariklo and its rings. Using X-Shooter at VLT we obtained a new reflectance spectra, here we compared this new set of data with the ones available in the literature. We showed how the water ice feature is visible in 2013 in accordance with the ring configuration, which had an opening angle of nearly 34° in 2013. Finally we also used models of the scattering of light to fit the visible and near-infrared spectra showing different characteristics to obtain information on the composition of Chariklo and its rings.

Results. We showed that past absolute photometry of Chariklo from the literature and new photometric data that we obtained in 2013 can be explained by a ring of particles whose opening angle changes as a function of time. We used the two possible pole solutions for the ring system and found that only one of them, $\alpha = 151.30 \pm 0.5^\circ$, $\delta = 41.48 \pm 0.2^\circ$ ($\lambda = 137.9 \pm 0.5^\circ$, $\beta = 27.7 \pm 0.2^\circ$) provides the right variation of the aspect angle with time to explain the photometry, whereas the other possible pole solution fails to explain the photometry. From spectral modeling, using the result on the pole solution, we derived the composition of Chariklo surface and of that of the rings. Chariklo surface is composed by nearly 60% of amorphous carbon, 30% of silicates and 10% of organics, no water ice was found on the surface. Whereas the ring contains 20% of water ice, 40-70% of silicates and 10-30% of tholins and small quantities of amorphous carbon.

Key words. Kuiper belt objects: individual: (10199) Chariklo. Planets and satellites: rings

1. Introduction

Centaur objects are thought to be objects that originated in the trans-Neptunian region and that are currently in a transition phase, with unstable orbits lying between Jupiter and Neptune and dynamical life-times of the order of 10 Myears (Horner et al. 2004). They can become short period comets, and in fact, several Centaurs have already shown cometary-like activity. The first object of this class with cometary activity ever discovered was (2060) Chiron (Tholen et al. 1988). Some time after its discovery it experienced a brightness outburst, developed a coma and showed typical cometary behavior. Another relevant object among the Centaurs is (10199) Chariklo, which appears to be the largest object in this population with a diameter of 248 ± 18 km (For-

nasier et al. 2013; Duffard et al. 2014), but contrary to Chiron, has never shown any traces of cometary activity. A vast photometric monitoring along a large time span has been made since its discovery in 1997, trying to identify possible outbursts, but no such potential outbursts have been identified thus far (e.g. Belskaya et al. 2010).

Recently, the observation of a multi-chord stellar occultation reported in Braga-Ribas et al. (2014) revealed the presence of two dense rings around Chariklo, with widths of about 7 and 4 km, optical depths of 0.4 and 0.06, and orbital radii of 391 and 405 km, respectively.

In the compilation of the photometry by Belskaya et al. (2010) the absolute magnitude of Chariklo increased with time (Chariklo's brightness decreased) from 6.8 in 1998 to 7.4 in 2009 and this has been interpreted by some authors as a possible hint for a decreasing comet-like activity in this body (Guilbert et al. 2009b; Belskaya et al. 2010) which seemed reasonable because several other centaurs are known to have cometary-like activity (Jewitt 2009), not only Chiron. Nevertheless, Guilbert-Lepoutre (2011) showed with independent arguments that it is currently

[★] Partially based on observations collected at the European Organization for Astronomical Research in the Southern Hemisphere, Chile. DDT 291.C-5035(A). Based on observations carried out at the Complejo Astronómico El Leoncito, operated under agreement between the Consejo Nacional de Investigaciones Científicas y Técnicas de la República Argentina and the National Universities of La Plata, Córdoba, and San Juan.

not possible a cometary activity for Chariklo, unless an additional energy source is provided to the object (through an impact for example).

On the other hand, several independent spectroscopic studies of Chariklo reported the detection of water ice absorption bands located at 1.5 and 2.0 μm (e.g. Brown et al. 1998; Brown & Koresko 1998; Dotto et al. 2003). Later in time, observations with higher S/N ratio show an albedo that has not signs of the presence of water ice (Guilbert et al. 2009a,b). In this work the authors tried to explain the observed spectral variations in terms of surface heterogeneity which was at the moment a plausible explanation.

However, in the light of the recent discovery by Braga-Ribas et al. (2014) there is another option to explain the photometry: Chariklo's dimming and the overall photometric behavior of Chariklo is related to the change in the aspect angle of a bright and dense ring system around Chariklo.

A dense ring system is also a natural source that could explain the changes in the depth of the water ice feature observed in Chariklo's spectrum, like in Saturn's ring (Hedman et al. 2013). Moreover, the fact that there is one spectrum that shows no indication of water ice suggests that all the water ice detected on Chariklo would not be on Chariklo's surface but on its rings. One of the ring pole positions derived by Braga-Ribas et al. (2014) implies that the rings were seen edge-on in 2007-2008 when no water ice spectral features were observed in Chariklo (Guilbert-Lepoutre 2011). Our interpretation also predicts that water ice features should already be detectable in 2013. To confirm that, here we present spectroscopic observations taken with the 8m VLT using X-Shooter that clearly show the reappearance of the water ice spectral features in the NIR.

In summary, Braga-Ribas et al. (2014) show the detection of the ring system through stellar occultation and we present here evidence for the ring system based on photometry and spectroscopy. We also derive additional constraints to the rings properties that are not directly obtained from the occultation. In section 2, the new observational data are presented and the analysis of the data is presented in section 3. Finally, the discussion is shown in section 4 and conclusions in section 5.

2. New observational data

With the intention to obtain new values for the absolute magnitude of Chariklo, photometric observations were made with different telescopes in 2013. Also, as was mentioned, a reflectance spectra in the vis+nir range was obtained with the X-Shooter at VLT.

2.1. Imaging

Observations with the Cerro Burek 0.45m ASH telescope in Argentina, the San Pedro de Atacama 0.4m ASH2 telescope in Chile and the 1.54m Bosque Alegre telescope in Argentina were made in different dates through May and June 2013. The exact observing dates at each telescope and other relevant information are summarized in table 1. The observations consisted in CCD images taken with different cameras. Average seeing was 2 arcsec at ASH, 2.5 arcsec at ASH2 and 2.1 arcsec at Bosque Alegre. The images were acquired with no filter in order to maximize the signal to noise ratio. Synthetic aperture photometry was obtained using apertures diameters two times larger than the seeing. Because the sensitivity of the CCD cameras peaked in the R band, absolute photometry was made using the R magnitudes of

UCAC2 reference stars of similar color to that of Chariklo. This yields magnitudes with an uncertainty of around 0.15 mag. We used large sets of images in order to average out possible rotational variability of Chariklo. The R magnitudes obtained at each telescope were corrected for geocentric (Δ) and heliocentric (r) distance applying $-5\log(r\Delta)$ where r and Δ are in astronomical units. The R magnitudes were translated into V magnitudes by using the known V-R color of Chariklo (0.48 ± 0.05) and also, phase angle corrections were applied with a 0.06 mag/degree slope parameter (Belskaya et al. 2010). The absolute magnitude obtained in June 2013 are 7.01 ± 0.12 mag, 7.00 ± 0.13 mag and 7.16 ± 0.18 mag for ASH2, ASH and Bosque Alegre, respectively. For May 2013 observations at ASH gives $H_V=6.91\pm 0.15$ mag. These new results are shown in Figure 1 also with the compilation of the literature value. The explanation on how the model was obtained is given below in Section 3.2.

2.2. Chariklo Reflectance Spectra

We obtained a reflectance spectrum of Chariklo ranging from 0.5 to 2.3 μm using the X-Shooter¹ spectrograph located in the Cassegrain focus of unit 2 at the VLT. X-Shooter is an *echelle* spectrograph that can simultaneously record all the spectral range by means of two dichroics that split the incoming beam from the telescope and send it to three different arms: UVB ($\approx 0.3 - 0.5 \mu\text{m}$), VIS ($\approx 0.5 - 1.0 \mu\text{m}$), and NIR ($\approx 1 - 2.4 \mu\text{m}$).

Chariklo was observed on the night of August 3rd, 2013. We used the SLIT mode. The slits chosen were 1.0, 0.9 and 0.9 arcsecs for the UVB, VIS, and NIR arms respectively, yielding a resolving power of about 5000 per arm. To eliminate the sky contribution from the NIR frames we nodded the telescope. Unfortunately X-Shooter does not yet allow nodding only in the NIR arm. We also observed a star to be used as both telluric and solar analog (HD144585). All data were reduced using the X-Shooter pipeline, following the procedure described in Alvarez-Candal et al. (2011), which includes flat-fielding, wavelength calibration, and merging of different orders. The data were wavelength and spatially calibrated by creating a two-dimensional wave-map, necessary because of the curvature of the Echelle orders. Then we extracted the one-dimensional spectra using IRAF, which proved better than using the one-dimensional spectra provided by the pipeline, and we divided those of Chariklo by the corresponding star. Finally, a median filter was applied to remove remaining bad pixels. In Figure 2 we show the spectrum of Chariklo from 0.5 up to 2.3 μm obtained in August 2013 with X-Shooter.

3. Analysis of the data

3.1. Analysis of the spectrum

The spectrum of Chariklo taken in 2013 shows a red slope in the visible of 9.375%/1000 \AA from 0.55 to 0.75 μm . This slope is typically related with the presence of complex organics on the surface of the body although it has also been related in the outer solar system to the presence of amorphous silicates e.g. the reddish slope of trojans asteroids (Emery et al. 2011). It also shows two clear absorption bands centered at 1.5 and 2 μm typical of water ice. To study the variation on the reflectance from Chariklo's surface we compared the parameters of this spectrum (spectral slope in the visible and 2.0 μm band depth) with others in the literature (see table 2). However, this comparison has to

¹ <http://www.eso.org/sci/facilities/paranal/instruments/xshoot>

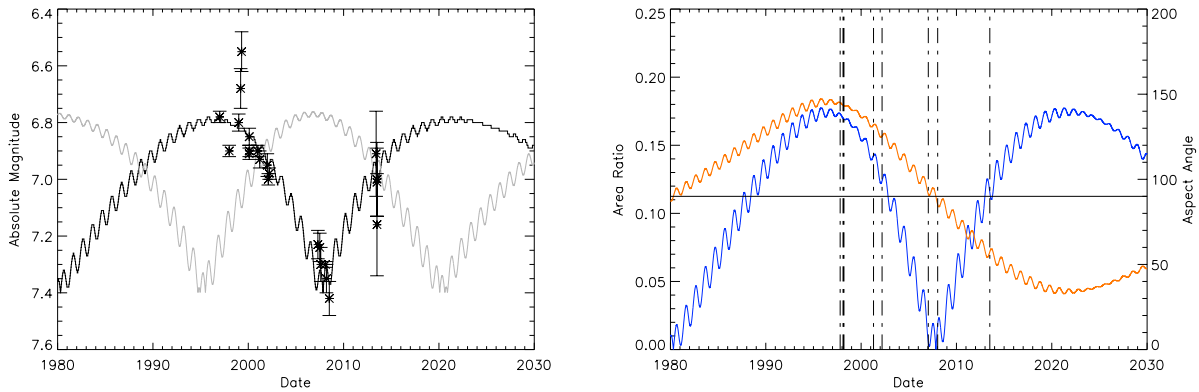


Fig. 1. Left panel: Variation of the H_V during time. Data taken from Belskaya et al. (2010) and our own observations. The solid curve represents the model described by Eq. (1). It is fitted to the data, assuming the ring pole position mentioned in the text ($\lambda = 138$, $\beta = 28$). We assume that Chariklo’s rotation axis is aligned with ring pole. The right panel show the variation of the aspect angle with time (orange line, scale at right). As can be seen the aspect angle is 90° in the period 2007-2008. Also presented in this panel the variation of the area ratio (blue line, scale at left). Vertical lines are the dates when reflectance spectra were taken. The area of Chariklo was considered to be the one of an ellipsoid with axis $a=122\text{km}$, $b=122\text{km}$, $c=117\text{km}$. The area of the rings were calculated with the parameters taken from Braga-Ribas et al. (2014).

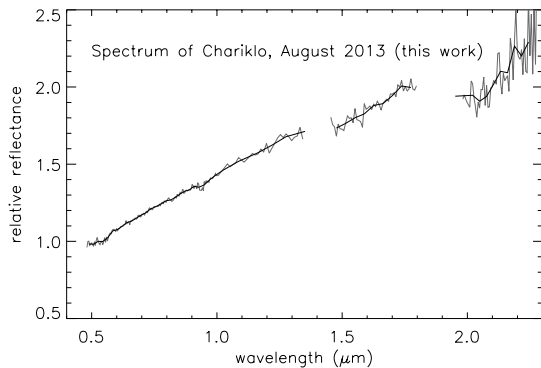


Fig. 2. Reflectance spectra of Chariklo obtained in August 2013 using the X-Shooter at VLT.

Table 1. Observational conditions for the images to obtain the reported absolute magnitudes and for the new Chariklo spectra obtained with X-Shooter at VLT.

Photometry			
Object	Telescope	exptime (s)	Filter
Chariklo	ASH	300	Luminance
Chariklo	ASH2	300	Luminance
Chariklo	Bosque Alegre	300	Clear
Near-infrared spectra			
Object	exptime (s)	airmass	arm
Chariklo	4×530	1.035-1.054	UVB
	4×560		VIS
	4×600		NIR
HD144585	2×0.8	1.022-1.023	All

be taken with care. Nowadays observational techniques of Centaurs and trans-Neptunian objects are pretty standard and solar analogues are widely used to remove the signature of the Sun in the reflected light from the body. However, this was not always done in the decade of the 90s e.g. in the library of spectra of Chariklo that we are using Brown et al. (1998) used the spectrum of a C-type asteroid and Brown & Koresko (1998) used the

black body function of an A2-type star divided by that of the sun. Both methods are acceptable but they can affect the slope of the continuum.

For our study visible slopes for all the spectra (the new spectrum presented here and those from the literature) were computed using a linear fit to the data between 0.55 and $0.75 \mu\text{m}$. After normalizing all of them at $0.55 \mu\text{m}$. To count for the error several fits were ran randomly removing points from the input data, the slope was chosen as the average value while the standard deviation was chosen as the error.

Band Depths (%) were computed (also for all the existing spectra) by defining a linear continuum between 1.75 and $2.2 \mu\text{m}$ and then measuring the reflectance at $2.0 \mu\text{m}$ relative to the one at $1.75 \mu\text{m}$. The determination of the band depth has the problem that the band is near a large telluric absorption which leaves considerable residuals after correction. This might have some incidence on the measured values.

3.2. Analysis of the photometric data

To make an interpretation of the photometry compiled by Belskaya et al. (2010) and our new photometry during 2013, we built a model of the reflected light by the main body and a model of the reflected light by the rings. For the main body we obtained the flux by multiplying the projected area of an ellipsoid by the geometric albedo of Chariklo.

The total flux density F_{tot} coming from both Chariklo and its rings is then given by:

$$\frac{F_{tot}}{F_{sun}} = A_p p_v f(\alpha) + p_v^{R1} 2\pi W_1 a_1 \mu f^{R1}(\alpha) + p_v^{R2} 2\pi W_2 a_2 \mu f^{R2}(\alpha) \quad (1)$$

Where A_p is the projected area of Chariklo, p_v is the geometric albedo of the main body, p_v^{Ri} are the geometric albedo of the rings, W_i is the radial width of the rings, a_i is the radial distance of the ring to the main body, μ is the absolute value of the cosine of the aspect angle as seen from Earth, while the phase functions $f(\alpha)$ for the main body and rings are assumed to be equal to unity. This is a good approximation because the phase slope parameter of Chariklo and other centaurs is very small, only around 0.06mag/degree and the phase angle variation of Chariklo is only

Table 2. Visible spectral slope and NIR absorption band depth for all the spectra obtained in literature and the one presented here.

Visible spectra				
date	slope	sigma	aspect angle	reference
1998-03	3.82	0.45	142	(1)
2007-03	7.27	0.73	91	(2)
2008-02	10.36	1.04	83	(3)
2013-06	9.38	0.94	58	this work
Near-infrared spectra				
date	depth [%]	sigma	aspect angle	reference
2013-06	11.40	8.57	58	(this work)
2008-02	3.97	2.50	83	(3)
2007-03	1.36	2.68	91	(2)
2002-03	4.40	1.84	125	(4)
2001-04	15.24	2.86	132	(4)
1998-03	7.67	3.59	142	(5)
1997-10	6.97	4.84	144	(6)

References. (1)Barucci et al. (1999); (2)Alvarez-Candal et al. (2008); (3)Guilbert et al. (2009a); (4)Dotto et al. (2003); (5) Brown & Koresko (1998); (6)Brown et al. (1998)

around 3° . The parameters W_i and a_i were taken from fits to the occultation profiles by Braga-Ribas et al. (2014). The geometric albedo of Chariklo p_V was taken from Fornasier et al. (2013). We need to mention here that the Fornasier et al. (2013) observations with the Herschel Space Telescope were taken during August 2010, where the aspect angle was close to 50° , and the area of the ring over the area of Chariklo was 0.08. In the albedo determination they use $H_{mag} = 7.4 \pm 0.25$, that was transformed into an albedo with a conservative error which covers the selected H_{mag} for that date. The obtained albedo with its error was used in our modeling.

The free parameters of the model are the area of Chariklo and the albedo of the rings. The parameter A_p depends on the ring pole orientation and on the shape of the body. For the spin axis orientation we used the one preferred given in Braga-Ribas et al. (2014), that gave satisfactory results in agreement with the photometry. These values correspond to $\lambda = 138^\circ$, $\beta = 28^\circ$. The nominal shape used is an ellipsoid whose projected shape matches that observed in the stellar occultation.

Using the pole determination and size estimated from the stellar occultations in Chariklo, we applied the equations presented in Tegler et al. (2005) to obtain the evolution of aspect angle, and applied eq. 1 to get absolute magnitudes. The first results that can be seen on these plots is when the ring plane is crossing the observers (equatorial view or aspect angle = 90°). That happens in 2007-2008 for Chariklo as can be seen in Figure 1, right panel (blue curve, scale at right). The other pole solution gives results that are not compatible with the photometry as you can see in Figure 1 (left panel, dotted line).

The evolution of the aspect angle can be seen in Figure 1 (right panel) from 1980 to 2030. The vertical lines represents when the different reflectance spectra were taken (Table 2). The latest spectrum obtained with X-Shooter in August 2013 has an aspect angle of 58° , close to the Brown & Koresko (1998) spectra on 1998. We also plot in figure 1 the area ratio between rings and Chariklo. It is evident that the best time to see only the contribution of Chariklo, when the rings were edge-on, was during 2007-2008, while all the others have some exposed area from the rings.

3.3. Spectral modeling

As mentioned before, there are several spectra of Chariklo in the literature (Guilbert-Lepoutre 2011, and references therein). These spectra show some similarities and differences that have been interpreted as surface heterogeneity on Chariklo, as the ring system was not known. All the visible spectra are red, what suggests the presence of some organics and/or silicates on the surface. Almost all the NIR spectra show absorptions very similar to those of water ice neither at 1.52 and/or $2.02 \mu\text{m}$. However one of the spectra does not show any trace of water ice absorption at 1.52 nor at $2.02 \mu\text{m}$.

Our goal in this section is to study if the variation on the spectra of Chariklo can be explained based on the different exposure of the rings depending on the aspect ratio instead of based on compositional heterogeneity on the surface of the centaur.

We used the Shkuratov theory (Shkuratov et al. 1999) to generate a collection of synthetic spectra that reproduce the overall shape of the spectrum of the whole system: Chariklo and rings. These models use as input the optical constants, the relative abundance and the size of the particles of different materials to compute the geometric albedo of the surface at different wavelengths. These approximation has been widely used to interpret the surface composition of minor icy objects in the Solar System (Pinilla-Alonso et al. 2007; Merlin et al. 2010; Poulet et al. 2002). In spite of their impressive history of success, ambiguous results are derived in some cases and have to be taken with care, as none of the solutions are unique.

To reduce this ambiguity we put special emphasis on the reproduction of the two most representative characteristics of these spectra, the red slope from the visible to the NIR and the two water ice bands. To do that we chose spectra that cover visible and NIR, or at least J, H and K bands. If the data at different wavelengths come from different observations we chose only those that are close in time so that the overall shape of the spectrum is not affected by the variation in the aspect angle. With this approach, we have tried to minimize the possibility of misinterpretation.

In the rest of the section we will follow this approach: First, we will model the surface of Chariklo using the spectra that has the smallest contribution from the rings. Second we will constrain the composition of the rings on different dates to show that the origin of the spectral variability is the geometric configuration of the system Chariklo + rings.

Modeling of the surface of Chariklo

As we want to constrain the composition of the surface of Chariklo we need a spectrum with a minimum contribution from the rings. The first spectrum that we modeled was that from Guilbert et al. (2009a) acquired in 2007 when according to our photometric model the aspect angle was 90.4° , as can be seen on Figure 1 right panel. This means that at this time almost all the light was scattered by Chariklo's surface, as the rings were seen by the edge and they are probably very thin. Based on our previous works (e.g. Licandro & Pinilla-Alonso 2005; Lorenzi et al. 2014) we did some tests to reproduce the shape of the spectrum with materials that are typically found on the surface of centaurs and trans-Neptunian objects (TNOs): water ice, complex organics (Triton, Titan, and Ice tholins), amorphous olivine, and amorphous pyroxene, with different content of magnesium and iron, and amorphous carbon.

Finally, as some of the spectra from Chariklo suggest the presence of water ice on the surface of the main body we de-

Table 3. Characteristics of the models of the continuum.

material	abundance (%)	size (μm)	reference
water ice	0 – 100	5 - 80	(1)
triton tholin	0 – 100	5 - 80	(2)
olivine	0 – 100	10 - 160	(3)
pyroxene	0 – 100	10 - 160	(3)
amorphous carbon	0 – 100	fixed 100	(4)

References. (1)Warren (1984); (2)McDonald et al. (1994)(3)Dorschner et al. (1995);(4)Rouleau & Martin (1991).

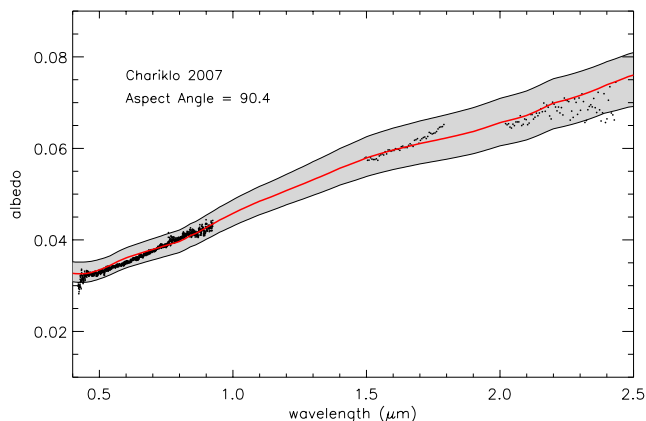


Fig. 3. Spectral model of the system Chariklo + rings with the rings on edge. The red line represents the best-fit to the spectrum (see table 4 for details). The shaded area represents a set of the 30 best fits to the spectrum. The relative reflectance is normalized to the albedo value of each model at $0.55 \mu\text{m}$ for the fit, this albedo value is allowed to vary between 0.035 and 0.041 (see text for details).

cided to include also water ice in the mixture. The details of the modeling and the references for the optical constants of the different materials are shown in table 3.

Also we used the estimated value of the albedo of Chariklo in the visible to constrain the number of solutions. We selected only the models with an albedo at $0.55 \mu\text{m}$ between 3.5% and 4.1% (according to the published estimations of the albedo (Fornasier et al. 2013)). For the evaluation of the χ^2 we normalize the spectrum to the value of the model at $0.55 \mu\text{m}$.

The final number of components in the mixture were determined by the fit. To chose the best fits we ranked the results using a χ^2 test. From the grid of models we selected a sample of 30, these are the models that according to the value of χ^2 are statistically equivalent with a 90% confidence (Press et al. 1992). Figure 3 shows the one with the lowest χ^2 value that we call the best fit (see table 4). We can also see the range of variation of these 30 models represented by the gray area around the fit. Remember that for each fit the spectrum is normalized to the value of the albedo at $0.55 \mu\text{m}$ and that we allow some range of variation for the albedo based on thermo-physical estimations of its value.

In next steps we will use this set of models for Chariklo as the canonical composition of the surface of the centaur without the influence of the rings, this is what we will call thereafter the *model of the continuum*.

Modeling of the rings

Now that we have the composition of the surface of Chariklo, the aim is to model the composition of the rings. In a second step we modeled the new spectrum presented in this work. This particular spectrum has the best characteristics for the modeling as it was acquired from 0.5 to $2.3 \mu\text{m}$ in only one shot using X-Shooter. It is also a good choice because it was acquired at an aspect angle of 58° showing clear traces of water ice. For the modeling of this spectrum we used “areal mixtures” of the *model of the continuum* with a grid of intimate models created in step one.

In the areal mixture we used the aspect angle of the rings to calculate the relative contribution of Chariklo and the rings to the total scattered light in the spectrum.

The final albedo from the model will be:

$$A_{Ch} \cdot (\text{model continuum}) + A_{rings} \cdot (\text{model rings})$$

where A_{Ch} and A_{rings} will be the relative normalized area of the centaur and the rings respectively. $A_{rings} = 1$ is viewing the ring face-on. This area ratio is taken from the photometric model. For example, for this particular case, the spectrum of 2013, the contribution from the rings and centaur is 0.144/0.853, respectively.

There are two different estimations of the albedo of Chariklo in the literature: Fornasier et al. (2013) find a value of $3.50 \pm 1.1\%$ while Stansberry et al. (2008) estimate a value of $5.73\%^{+0.49}_{-0.42}$. Now we know that the differences between these values are influenced by the different geometry of the Chariklo+rings system. Different geometry causes a variation in the absolute magnitude which is an important factor in the determination of the albedo. For that reason, in our models we allow the albedo to vary over all the range from 3.5 to 6.4%. Finally we ranked the best models using a χ^2 test and we select the collection of models that are statistically equivalent. In Figure 4 we show an example of how the modeling works. The details of the best model are shown in table 4. All of our best models for the rings include a 20% of water ice and an 80% of other materials intimately mixed to give the spectrum its overall reddish appearance. We will discuss these results in detail in the next section.

As a final test we study if the presence of crystalline water ice, instead of amorphous water ice, could improve the results. We found that the value of the χ^2 is slightly better when we use crystalline water ice, but the improvement is not significant. These tells us that from the signal to noise of the spectrum we cannot discard the presence of crystalline water ice.

In the last step we modeled other spectra from the literature. From the modeling presented above it is obvious that the overall shape of the spectrum from 0.5 up to $2.3 \mu\text{m}$ is very important. Based on the spectral coverage not all the spectra of Chariklo in the literature are good for this effort. We chose spectra with the best spectral coverage in the visible and near infrared and/or simultaneous in time. First we chose the spectrum from Dotto et al. (2003) obtained in 2002. This spectrum was acquired using the high-throughput low resolution mode of the Near-Infrared Camera and Spectrometer (NICS) at the Telescopio Nazionale Galileo (Baffa et al. 2001), this instrument incorporates an Amici prism disperser that yields a $0.8 - 2.5 \mu\text{m}$ spectrum in one only shot. So it provides a reliable shape of the continuum over a broad part of the wavelength range of our interest. The aspect angle was 125° showing a good percentage of the total area of the rings. We also model the spectrum presented in Guilbert et al. (2009b) that was obtained in 2008 and presented an aspect an-

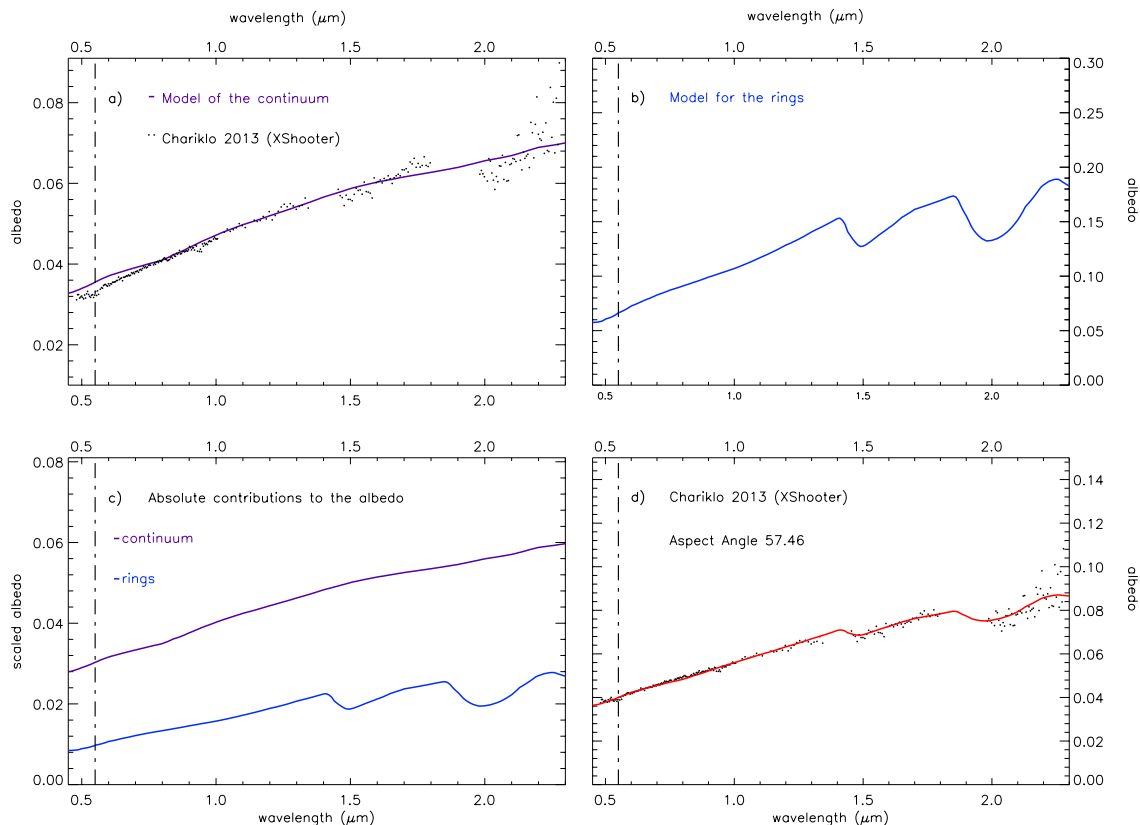


Fig. 4. Modeling of the spectrum of Chariklo + rings in 2013: a) Model of the continuum superimposed to the observed spectra in 2013; b) Model for the rings; c) Absolute contribution of each part, continuum and rings; d) Final model for the spectrum of the system in 2013.

gle of 83° . This spectrum combines two sets of data acquired in February 2008. One set covers the visible wavelengths from 0.4 up to $1.0\ \mu\text{m}$, while the other covers H and K band in the NIR. These data were merged together using photometry at V, R, I, J, H and K bands (see Guilbert et al. (2009b) for details). All this procedure results in a spectrum that is adequate for the modeling effort. In 2008 the ratio of the area of the rings and Chariklo exposed was 0.03/0.97 respectively, while in 2002 it was 0.151/0.849. The aspect angle for 2008 was 83° and 125° for 2002.

We used again areal mixtures of the *model of the continuum* and the same grid of models that we used for the composition of the rings. We selected the best model as we did before. These models are shown in Figure 5 together with the models for 2007 (continuum) and 2013 for comparison. They are shifted in the vertical for clarity. The details of the models are included in table 4.

Results from the modeling

In table 4 we show the best model selected from our fits to the spectra of Chariklo and its rings at different aspect angles. These were selected using a χ^2 criterium. However these models may not be unique in its goodness of fit as they rely on the assumptions inherent to the Skhuratov formalism, as well as on the materials present in the modeling. Each observed spectrum can be fitted by a collection of models that are statistically equivalent. The absence of features in the reflectance of some of the surface

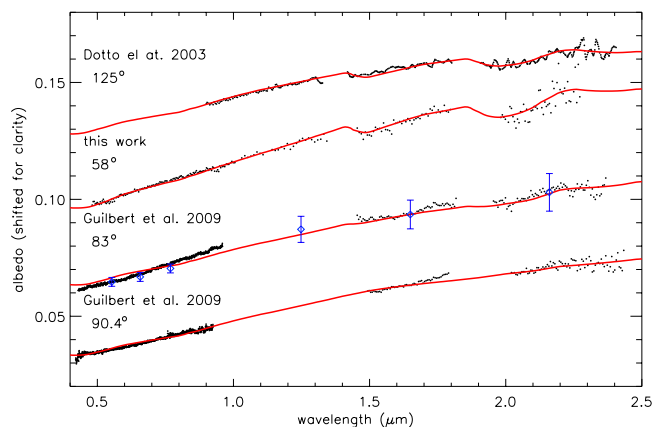


Fig. 5. Models for a set of spectra showing variability. Parameters are shown in Table 4. Each spectrum is labeled with the reference and the aspect angle of the system of rings at the date of the observations.

components increases the degree of degeneracy of the solutions. However, these materials are necessary to fit the overall red slope of the continuum. Other materials, such as the water ice are better constrained due to the presence of two absorption bands in the wavelength range of study. Nonetheless, the models selected provide insight into the surface of Chariklo and the rings. In this section we expose the main results that we get from the modeling effort.

One of the main results in the modeling comes from the spectrum acquired in 2007, when almost all the light is scattered by Chariklo's surface. Our best models all discard the presence of water ice on the surface of the centaur. They also show that this surface is composed of a mixture of amorphous silicates (30%), red-complex organics (10%) and amorphous carbon (60%). The mixture of these materials is what gives the spectrum its reddish featureless appearance.

The second main result is the fact that we can model all the other spectra with a canonical composition for the continuum linearly combined with a canonical composition for the rings, but changing their relative contributions by means of the aspect angle of the system. The rings can contain up to a 20% of water ice (with a size particle of $\sim 100 \mu\text{m}$) and the best selected models fits bands in the three spectra with very different shape, from the very shallow in the spectrum from 2008 (aspect angle = 83°) to the deeper in the spectrum of 2013 (aspect angle = 58°)

These models clearly discard a composition of the rings dominated by water ice.

However, although the composition of Chariklo and the non-icy components in the rings is pretty similar, it also shows some differences that are important to note, the most evident is the abundance of amorphous carbon that seems to be much larger on the surface of Chariklo than on the rings. This could be an indication that the ring is younger than the surface of the centaur that exhibits a composition more similar to that of highly processed cometary nuclei (Campins et al. 2006). The rings are supposed to be formed by small particles that have collisions with each other, this process can expose the water, showing a younger surface than the main body.

From the results of the modeling we can also have a broad estimation of the albedo of the rings. Revising the albedo at $0.55 \mu\text{m}$ of all the best fits we estimate a value of $7.0 \pm 1.0\%$ for the albedo of the rings (panel b in Figure 4). At the same time the albedo of Chariklo remains pretty low at $\sim 3.6\% \pm 1.0\%$ (panel a in Figure 4). It is when we scale these albedos considering the aspect angle (panel c) when we get the final contribution to the total albedo of the system Chariklo + rings of $\sim 4.0\% \pm 1.0\%$.

While the size of water ice particles is well constrained, the size of the particles for the other components is more degenerated. This is because there are not absorption bands of these materials in the wavelength range of the study and all of them can be combined in different ways to produce a featureless reddish and low albedo final spectrum similar to that of Chariklo.

We need to mention here that the size of the particles that we obtained do not correspond to a detailed description of the distribution of the size of the particles in the rings. The ring could also be populated with larger chunks of material but covered with fine grained material with the sizes we found in our modeling.

4. Discussion

The key point to obtain all the results presented in our work is the determination of the spin axis of Chariklo. This was done from the stellar occultation reported by Braga-Ribas et al. (2014) and assuming that the rings are in the equatorial plane of Chariklo. The spin axis orientation that can explain the absolute magnitudes observed in the 1997-2013 period and also explains the spectroscopy as already stated in the introduction, is consistent with one of the two spin axis orientations derived from the stellar occultation reported by Braga-Ribas et al. (2014). But this orientation also explains the lack of detection of a rotational lightcurve in the 1997-2000 time frame (e.g. Peixinho et al.

2001), because at that time the aspect angle was nearly 140 degrees so a triaxial ellipsoid or a very irregular body or a body with albedo variegations on its surface would produce nearly flat rotational light curves. Belskaya et al. (2010) already pointed out this possibility and provided a tentative spin axis orientation that turned out to be off by around 30 degrees, which is remarkable given the information available at that time.

The spin axis orientation in our model can also explain why a rotational lightcurve has been detected in 2013 from high signal to noise images with an amplitude of 0.1 mag Fornasier et al. (2014) and a period of 7.004 ± 0.036 hours. As shown in fig 1 the aspect angle in 2013 is large enough to allow revealing rotational variability. A triaxial ellipsoid with axes dimensions $a \sim 122 \text{ km}$, $b \sim 122 \text{ km}$, $c \sim 117 \text{ km}$ can reproduce the observed rotational amplitude in 2013 and the non-detection in 1997-2010 if all the variability is due to shape.

The correct spin axis orientation not only must explain the rotational lightcurve of Chariklo and the absolute magnitude variability but also the spectral behaviour over time. Our modeling shows that we can explain the changes in the spectrum of Chariklo, and in particular, the shape of the bands of water-ice, by means of changes in the aspect angle of a system formed by a main body and a system of rings. By modeling the spectrum acquired in 2007 we also discard the presence of water ice on the surface of Chariklo. Moreover, the fact that on this date, when the rings were edge-on we did not see any trace of water ice in the spectrum from the system suggests that the rings must be thin.

This shape of Chariklo is not far from a Maclaurin ellipsoid of density $\sim 750 \text{ kg/m}^3$ spinning at 8h, using the equilibrium figures formalism (e.g. Chandrasekhar (1987), which would mean that Chariklo would not be far from hydrostatic equilibrium, and the derived density seems consistent with that of small TNOs. From the analysis of rotational lightcurves of a sample of TNOs and Centaurs, Duffard et al. (2009) concluded that most TNOs seemed to be in hydrostatic equilibrium and that this possibility also holds for the Centaurs, at least for the largest ones such as Chariklo. A detailed shape from rotational lightcurves and taking into account the occultation chords has been inverted by Carry et al. (private communication), although in that model all the variability is supposed to arise from shape, which is not necessarily the case, and the model does not include the effect of a ring which slightly decreases the amplitude of the rotational lightcurve when the aspect angle is not 90° .

Rings are common around the giant planets in the Solar System, however their appearance and composition is very different probably as a result of a different origin and the exposition to resurfacing mechanism acting at different degrees of intensity (Tiscareno 2013, for a review). This translates from rings formed by meter-centimeter size particles of almost pure water ice, to optically thin rings formed by micrometer-size particles of dust (silicates). The results of our modeling show that the rings of Chariklo are composed of a mixture of bright and dark material. The composition of the rings is more similar to what we would expect from the disruption of an object formed in the same region as Chariklo itself, with a mixture of ices, silicates and carbonaceous materials processed by high-energy irradiation. While part of the appearance of the rings of the giant planets is sculpted by the action of the electromagnetic forces generated by the planet itself, in the case of Chariklo we expect that most of the changes are produced by the action of micro-collisions. The area of Chariklo's rings is about $25\,000 \text{ km}^2$ and we can expect that, as it happens for the planetary rings, debris are continuously impacting the material on the ring causing changes in their orbit

Table 4. Characteristics of the best models of Chariklo and rings used in the figures. These best models were chosen from the collection of models that are statistically equivalent with a 90% confidence.

year	Concentration (%)					Particle Size (μm)					
	Water Ice	Tholin	Olivine	Pyroxene	Carbon	Water Ice	Tholin	Olivine	Pyroxenes	Carbon	
2007	0	10	20	10	60	5	10	210	60	100	
2013	cont	0	10	10	20	60	5	10	110	110	100
	ring	20	10	30	40	0	70	25	110	10	100
2008	cont	0	10	10	20	60	5	10	110	110	100
	ring	20	30	10	30	10	90	70	110	10	100
2002	cont	0	10	10	10	70	5	15	110	210	100
	ring	20	20	50	0	10	60	13	210	10	100

and composition. These continuous collisions would sublimate part of the ice exposed at the moment of the formation of the rings. They also are responsible for the fragmentation of the most fragile materials. Another important factor affecting the chemical composition of the grains is the irradiation by high-energy particles that processes the ices and causes the amorphization of water ice and the transformation of simple hydrocarbons into complex dark material as the carbon.

Due to the signal to noise of our spectra we cannot distinguish in the shape of the $1.5 \mu\text{m}$ band neither from the modeling the state of the water ice. Amorphous water ice is expected due to irradiation, but also crystalline water ice is expected due to the collisions of the fragments in the rings and to the micro-bombardment. We think that the ice is probably a mixture of the crystalline and amorphous state as it has been inferred in other bodies in the outer solar system (Pinilla-Alonso et al. 2009).

5. Conclusions

Using information on the pole of the rings from the 2013 stellar occultation:

- We prove that only one of the pole solutions found in Braga-Ribas et al. (2014) is compatible with the photometry and spectroscopy.
- We determined the times when the rings were edge-on and made the connection with the disappearance of the absorption band due to water ice on the spectra of Chariklo.
- We modeled the composition of Chariklo's surface that is 60% carbon, 30% silicates, and 10% organics and no water ice. We also model the composition of the rings that is 20% water ice, around 10 - 30% organics, between 40-70% on silicates and small quantities of carbon. With this modeling we discard the presence of water ice on the surface of Chariklo independently of the date of the observation. Also, we confirm that the spectroscopic variation is due to different area exposition of the rings not to variation of the surface of Chariklo itself.
- Except for the water, the composition of the rings is compatible with the same materials as the surface of Chariklo but combined in different relative abundances: Amorphous Carbon 0-20%; amorphous silicates 40-60%; organics 10-30%.
- The amount of water ice is well constrained by the models due to the presence of two absorption bands in the wavelength of study and has to be around 20% with a particle size $<100 \mu\text{m}$. As soon as the aspect angle is different from 90° the water ice band is visible again showing that a system of rings as the one detected for Chariklo, with 20% of water ice as the one inferred from our models, is evident in the NIR spectra at deviations of 10° or larger from the edge-on configuration.

Acknowledgements. RD acknowledge the support of MINECO for his Ramón y Cajal Contract. AAC thanks CNPq and FAPERJ for financial support. BS acknowledges support from the French grant ANR-11-IS56-0002 "Beyond Neptune II". FBR acknowledge the support of CNPq, Brazil (grant 150541/2013-9). Funding from Spanish grant AYA-2011-30106-CO2-O1 is acknowledged, as well as the Proyecto de Excelencia de la Junta de Andalucía, J.A.2007-FQM2998 and FEDER funds.

References

- Alvarez-Candal, A., Fornasier, S., Barucci, M. A., de Bergh, C., & Merlin, F. 2008, *A&A*, 487, 741
- Alvarez-Candal, A., Pinilla-Alonso, N., Licandro, J., et al. 2011, *A&A*, 532, A130
- Baffa, C., Comoretto, G., Gennari, S., et al. 2001, *A&A*, 378, 722
- Barucci, M. A., Lazzarin, M., & Tozzi, G. P. 1999, *AJ*, 117, 1929
- Belskaya, I. N., Bagnulo, S., Barucci, M. A., et al. 2010, *Icarus*, 210, 472
- Braga-Ribas, F., Sicardy, B., Ortiz, J. L., et al. 2014, *Nature*, 508, 72
- Brown, M. E. & Koresko, C. C. 1998, *ApJ*, 505, L65
- Brown, R. H., Cruikshank, D. P., Pendleton, Y., & Veeder, G. J. 1998, *Science*, 280, 1430
- Campins, H., Ziffer, J., Licandro, J., et al. 2006, *AJ*, 132, 1346
- Chandrasekhar, S. 1987, *Ellipsoidal figures of equilibrium* (New York : Dover, 1987.)
- Dorschner, J., Begemann, B., Henning, T., Jaeger, C., & Mutschke, H. 1995, *Astronomy and Astrophysics*, 300, 503
- Dotto, E., Barucci, M. A., Leyrat, C., et al. 2003, *Icarus*, 164, 122
- Duffard, R., Ortiz, J. L., Thirouin, A., Santos-Sanz, P., & Morales, N. 2009, *A&A*, 505, 1283
- Duffard, R., Pinilla-Alonso, N., Santos-Sanz, P., et al. 2014, *A&A*, 564, A92
- Emery, J. P., Burr, D. M., & Cruikshank, D. P. 2011, *AJ*, 141, 25
- Fornasier, S., Lazzaro, D., Snodgrass, C., & Alvarez-Candal, A. 2014, *A&A*, A15
- Fornasier, S., Lellouch, E., Müller, T., et al. 2013, *A&A*, 555, A15
- Guilbert, A., Alvarez-Candal, A., Merlin, F., et al. 2009a, *Icarus*, 201, 272
- Guilbert, A., Barucci, M. A., Brunetto, R., et al. 2009b, *A&A*, 501, 777
- Guilbert-Lepoutre, A. 2011, *AJ*, 141, 103
- Hedman, M. M., Nicholson, P. D., Cuzzi, J. N., et al. 2013, *Icarus*, 223, 105
- Horner, J., Evans, N. W., & Bailey, M. E. 2004, *MNRAS*, 354, 798
- Jewitt, D. 2009, *AJ*, 137, 4296
- Licandro, J. & Pinilla-Alonso, N. 2005, *ApJ*, 630, L93
- Lorenzi, V., Pinilla-Alonso, N., Licandro, J., Dalle Ore, C. M., & Emery, J. P. 2014, *A&A*, 562, A85
- McDonald, G. D., Thompson, W. R., Heinrich, M., Khare, B. N., & Sagan, C. 1994, *Icarus*, 108, 137
- Merlin, F., Barucci, M. A., de Bergh, C., et al. 2010, *Icarus*, 208, 945
- Peixinho, N., Lacerda, P., Ortiz, J. L., et al. 2001, *A&A*, 371, 753
- Pinilla-Alonso, N., Brunetto, R., Licandro, J., et al. 2009, *A&A*, 496, 547
- Pinilla-Alonso, N., Licandro, J., Gil-Hutton, R., & Brunetto, R. 2007, *A&A*, 468, L25
- Poulet, F., Cuzzi, J. N., Cruikshank, D. P., Roush, T., & Dalle Ore, C. M. 2002, *Icarus*, 160, 313
- Press, W. H., Teukolsky, S. A., Vetterling, W. T., & Flannery, B. P. 1992, *Numerical recipes in C. The art of scientific computing*
- Rouleau, F. & Martin, P. G. 1991, *Astrophysical Journal*, 377, 526
- Shkuratov, Y., Starukhina, L., Hoffmann, H., & Arnold, G. 1999, *Icarus*, 137, 235
- Stansberry, J., Grundy, W., Brown, M., et al. 2008, *Physical Properties of Kuiper Belt and Centaur Objects: Constraints from the Spitzer Space Telescope*, ed. M. A. Barucci, H. Boehnhardt, D. P. Cruikshank, A. Morbidelli, & R. Dotson, 161–179
- Tegler, S. C., Romanishin, W., Consolmagno, G. J., et al. 2005, *Icarus*, 175, 390
- Tholen, D. J., Hartmann, W. K., Cruikshank, D. P., et al. 1988, *IAU Circ.*, 4554, 2
- Tiscareno, M. S. 2013, *Planetary Rings*, ed. T. D. Oswalt, L. M. French, & P. Kalas, 309
- Warren, S. G. 1984, *Applied Optics*, 23, 1206